A shape optimization approach towards improving the understanding of magmatic plumbing system

Théo Perrot[1], **Freysteinn Sigmundsson**[2], **Charles Dapogny**[3]

[1]Mechanical engineering department, Ecole Normale Supérieure Paris-Saclay
[2]Institute of Earth Sciences, University of Iceland
[3]Jean Kuntzmann Institute, CNRS, Grenoble-Alpes University

Key Points:

- We present a novel approach to allow for assessment of volcanic magma domains shape based on level-set shape optimization.
- It relies on numerical finite element models iteratively modified to minimize the discrepancy to observed surface displacements
- We found strong dependence of best solution to initialization when benchmarked with synthetic data but application on data from Svartsengi 2022 inflation outputed relevant results.

Corresponding author: Théo Perrot, `theo.perrot@ens-paris-saclay.fr`

Abstract

In volcano geodesy, pressure sources in volcano roots responsible for surface movements are inverted using ground deformation data after defining a forward parametric model for the source. Such models are most of the time relying on predefined shape for the source, which can limit their accuracy. On the contrary, we propose here a shape optimization method to invert for pressure sources without any prior shape assumption. With that flexibility, the optimal shape of a pressurized magma body is determined by minimizing the discrepancy between observed and modelled displacement. We explore the capabilities of this approach with synthetic data first for validation and then apply it to observed ground deformation at the Svartsengi volcanic system in Iceland, demonstrating its potential to improve volcanic hazard assessment after maturation with further work.

Plain Language Summary

Enter your Plain Language Summary here or delete this section. Here are instructions on writing a Plain Language Summary: https://www.agu.org/Share-and-Advocate/Share/Community/Plain-language-summary

1 Introduction

In volcano geodesy, inverse problems are central to estimating the position of pressurized magma bodies at depth in volcano roots, using observed crustal deformation as a proxy. The displacement is measured by e.g. Global Navigation Satellite System (GNSS) point positioning, leveling campaigns, or interferometry analysis of synthetic aperture radar (InSAR) in a volcanic region (Dzurisin, 2007). The subsurface processes causing the movement are inferred from these observations. Magmatic sources are modeled as pressurized cavities that deform the surrounding host rocks and cause the surface to move. Various inversion methods based on parametric analytical or numerical models aim at finding the optimal values for the vector of d free parameters $\underline{m} \in \mathbb{R}^d$ of a model. An error function $J(\underline{m})$ is representative of the misfit between the observed displacements and the prediction of the model. $\underline{m}_{opt}$ can then be found using various inversion techniques minimizing J: global optimization based on analytic (Cervelli et al., 2001) or numerical models (Hickey & Gottsmann, 2014; Charco & Galán del Sastre, 2014), Bayesian inference (Bagnardi & Hooper, 2018; Trasatti, 2022), or genetic algorithms (Velez et al., 2011) on analytic models. The choice of the method can be influenced by what is feasible regarding the number of evaluations of $J(\underline{m})$: numerical models handle a complex description of the system, but are computationally expensive compared to analytic models, which on the other hand rely on strong simplifying assumptions (Taylor et al., 2021).

However, each of these finite-dimensional optimization methods is limited by the intrinsic assumption of a definite parametric shape for the source. In fact, analytic expressions can be derived for only a few regular shapes such as point source (Mogi, 1958), finite sphere source (McTigue, 1987), or ellipsoidal source (Yang et al., 1988), and any numerically generated shape must be parameterized to be inverted. A workaround would be an approach relying on shapes parameterized with more parameters, such as B-splines surfaces, to allow more exploration in the possible shapes. This implies optimization within a high-dimension domain, bringing unpleasant phenomena known as the curse of dimensionality. The goal of this paper is not to give a definitive answer to these limitations, but rather to lay the first stone for a new approach that overcomes these difficulties.

1.1 Shape optimization

Shape optimization generally aims to minimize a cost function depending on the domain. This practice is very popular in various disciplines, such as structural mechanics, where one typically wishes to improve the stiffness of a solid structure (Bendsoe & Sigmund, 2004), fluid mechanics, where it is applied to the design of pipes, heat exchangers or flying obstacles (Feppon et al., 2020), or again electromagnetism (Lucchini et al., 2022). Beyond academic investigations, it has aroused a tremendous enthusiasm in industry; nowadays, most Finite Element simulation and design softwares include a shape optimization module (Frei, 2015), (Slavov & Konsulova-Bakalova, 2019), (Le Quilliec, 2014). However, the use of these techniques in volcano geodesy is new to the best of our knowledge.

Multiple shape and topology optimization frameworks are available, see e.g. the review in (Sigmund & Maute, 2013). One popular strategy describes the design as a density function ρ on a large, fixed computational domain: ρ takes values 0 and 1 in the void and material regions, respectively, and intermediate values in between account for a fictitious mixture of both (Sigmund, 2001; Bendsoe & Sigmund, 2004). One major drawback of this approach is that it does not feature a clear representation of the boundary of the optimized design; in particular, approximations are needed to calculate physical quantities related to the domain at play. To alleviate this issue, we rely on a recent version of the Level Set method for shape optimization, which benefits from an explicit representation of the boundary at each step of the optimization.

2 Method

This section describes the considered shape optimization problem and its practical implementation. For a more complete mathematical background, we refer to e.g. (Allaire et al., 2021).

2.1 Presentation of the physical model

The region under scrutiny is represented by a fixed bounded domain $D \subset \mathbb{R}^3$, which writes as the disjoint reunion:

$$D = \Omega \cup \Omega^c, \text{ where } \Omega^c := D \setminus \overline{\Omega}.$$

In this setting, illustrated on Fig. 1 (a),

- The cavity $\Omega \Subset D$ stands for the magma chamber, whose shape is to be reconstructed. Its boundary $\Gamma = \partial\Omega$ is subjected to the force $\mathbf{f} = -\Delta P \mathbf{n}$, aligned with the unit normal vector $\mathbf{n} : \Gamma \to \mathbb{R}^3$ to Γ pointing outward Ω, and whose magnitude equals the (given) pressure difference ΔP between the cavity and the surrounding crust, see Section 5 for a discussion about this point.
- The complement Ω^c of Ω represents the surrounding Earth crust. It is filled by a homogeneous, isotropic elastic material. The displacement of the bottom side Γ_b of ∂D is set to $\mathbf{0}$ and the other boundary regions of D are free of stress.

The displacement $\mathbf{u}_\Omega : \Omega^c \to \mathbb{R}^3$ of the crust in these circumstances is the solution to the system of linearized elasticity:

$$\begin{cases} -\text{div}(Ae(\mathbf{u}_\Omega)) = \mathbf{0} & \text{in } \Omega^c, \\ \mathbf{u}_\Omega = \mathbf{0} & \text{on } \Gamma_\text{b}, \\ Ae(\mathbf{u}_\Omega)\mathbf{n} = \mathbf{f} & \text{on } \Gamma, \\ Ae(\mathbf{u}_\Omega)\mathbf{n} = \mathbf{0} & \text{on } \partial D \setminus \overline{\Gamma_\text{b}}, \end{cases} \tag{1}$$

where $e(\mathbf{u}) := \frac{1}{2}(\nabla \mathbf{u} + \nabla \mathbf{u}^T)$ is the strain tensor induced by a displacement $\mathbf{u}$ and A is the Hooke's law of crust material.

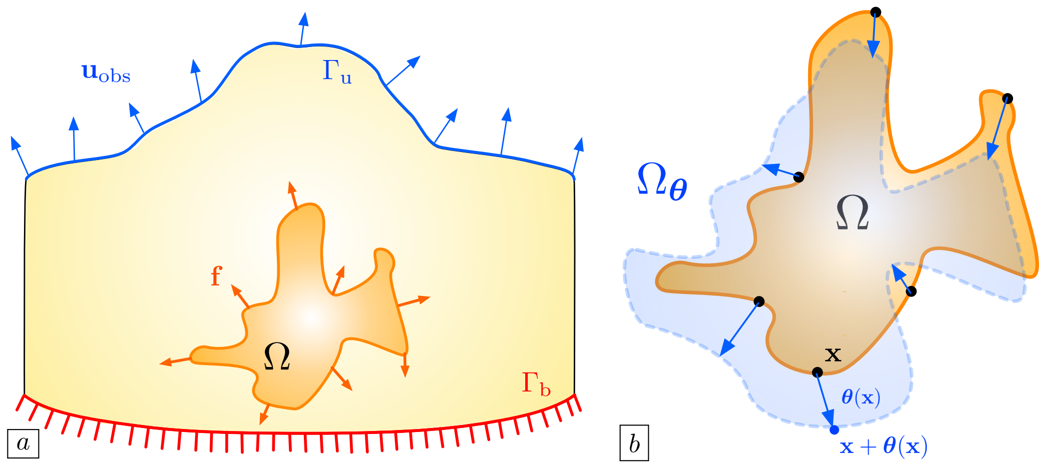

Figure 1. *(a) Sketch of the physical model; (b) Variation $\Omega_{\boldsymbol{\theta}}$ of Ω.*

2.2 Shape optimization for the reconstruction of the magma chamber

In the applications of this article, the shape Ω of the magma chamber is unknown. From the datum of observed values $\mathbf{u}_{\mathrm{obs}} : \Gamma_{\mathrm{u}} \to \mathbb{R}^3$ of the displacement of the crust on the upper surface Γ_{u} of D, we intend to identify Ω as the solution to the following shape optimization problem:

$$\min_{\Omega \subset D} J_{\mathrm{LS}}(\Omega), \text{ where } J_{\mathrm{LS}}(\Omega) := \int_{\Gamma_{\mathrm{u}}} |\mathbf{u}_\Omega - \mathbf{u}_{\mathrm{obs}}|^2 \, \mathrm{d}s, \tag{2}$$

featuring the least-square discrepancy between the prediction $\mathbf{u}_\Omega$ of the physical model (1), and the observed displacement $\mathbf{u}_{\mathrm{obs}}$ on Γ_u.

2.3 Shape derivatives

The solution of (2) calls for a notion of derivative for a function $J(\Omega)$ of the domain Ω. In this work, we rely on the boundary variation method of Hadamard, see (Allaire, 2006; Allaire et al., 2021; Henrot & Pierre, 2018; Murat & Simon, 1976). In short, variations of a reference domain Ω are considered under the form

$$\Omega_{\boldsymbol{\theta}} := (\mathrm{Id} + \boldsymbol{\theta})(\Omega), \text{ where } \boldsymbol{\theta} : \mathbb{R}^3 \to \mathbb{R}^3 \text{ is a “small” vector field,}$$

see Fig. 1 (b). The shape derivative $J'(\Omega)(\boldsymbol{\theta})$ of a function $J(\Omega)$ at Ω is the derivative of the underlying mapping $\boldsymbol{\theta} \mapsto J(\Omega_{\boldsymbol{\theta}})$, which produces the following expansion:

$$J(\Omega_{\boldsymbol{\theta}}) = J(\Omega) + J'(\Omega)(\boldsymbol{\theta}) + \mathrm{o}(\boldsymbol{\theta}), \text{ where } \frac{\mathrm{o}(\boldsymbol{\theta})}{||\boldsymbol{\theta}||} \xrightarrow{\boldsymbol{\theta} \to \mathbf{0}} 0. \tag{3}$$

In practice, $J'(\Omega)(\boldsymbol{\theta})$ is used to identify a descent direction $\boldsymbol{\theta}$, i.e. a vector field such that $J'(\Omega)(\boldsymbol{\theta}) < 0$. Intuitively, the perturbed shape $\Omega_{\tau\boldsymbol{\theta}}$ by such a descent direction for a “small enough” descent step $\tau > 0$ performs “better” than Ω in terms of the criterion $J(\Omega)$, i.e. $J(\Omega_{\tau\boldsymbol{\theta}}) < J(\Omega)$, see (3).

The calculation of the shape derivative of the functional $J_{\mathrm{LS}}(\Omega)$ in (2) is a tedious, but classical issue. It can be realized thanks to the adjoint method, see e.g. (Cea, 1986; Plessix, 2006) and (Allaire et al., 2004) in this particular mathematical context:

$$J'_{\mathrm{LS}}(\Omega)(\boldsymbol{\theta}) = \int_\Gamma v_\Omega \, (\boldsymbol{\theta} \cdot \mathbf{n}) \, \mathrm{d}s, \text{ where } v_\Omega := Ae(\mathbf{u}_\Omega) : e(\mathbf{p}_\Omega) + \Delta P \, \mathrm{div}(\mathbf{p}_\Omega), \tag{4}$$

and the adjoint state $\mathbf{p}_\Omega$ is the solution to the following problem:

$$\left\{\begin{array}{cl} -\mathrm{div}(Ae(\mathbf{p}_\Omega)) = \mathbf{0} & \text{in } \Omega^c, \\ \mathbf{p}_\Omega = \mathbf{0} & \text{on } \Gamma_\mathrm{b}, \\ Ae(\mathbf{p}_\Omega)\mathbf{n} = \mathbf{0} & \text{on } \partial D \setminus (\overline{\Gamma_\mathrm{u}} \cup \overline{\Gamma_\mathrm{b}}), \\ Ae(\mathbf{p}_\Omega)\mathbf{n} = -2(\mathbf{u}_\Omega - \mathbf{u}_\mathrm{obs}) & \text{on } \Gamma_\mathrm{u}. \end{array}\right. \tag{5}$$

The expression (4) paves the way to a natural descent direction for $J_{\mathrm{LS}}(\Omega)$:

$$\boldsymbol{\theta} = -v_\Omega\, \mathbf{n}. \tag{6}$$

2.4 Level-set representation

The magma chamber $\Omega \subset D$ is represented via the Level Set method, see e.g. (Osher & Fedkiw, 2006; Sethian, 1999), and the article (Allaire et al., 2004) about its introduction in shape and topology optimization. Briefly, Ω is described implicitly, as the negative region of a scalar, "level set" function $\phi : D \to \mathbb{R}$, see Fig. 2 (a).

$$\forall \mathbf{x} \in D, \quad \left\{\begin{array}{ll} \phi(\mathbf{x}) < 0 & \text{if } \mathbf{x} \in \Omega, \\ \phi(\mathbf{x}) = 0 & \text{if } \mathbf{x} \in \Gamma, \\ \phi(\mathbf{x}) > 0 & \text{if } \mathbf{x} \in \Omega^c. \end{array}\right. \tag{7}$$

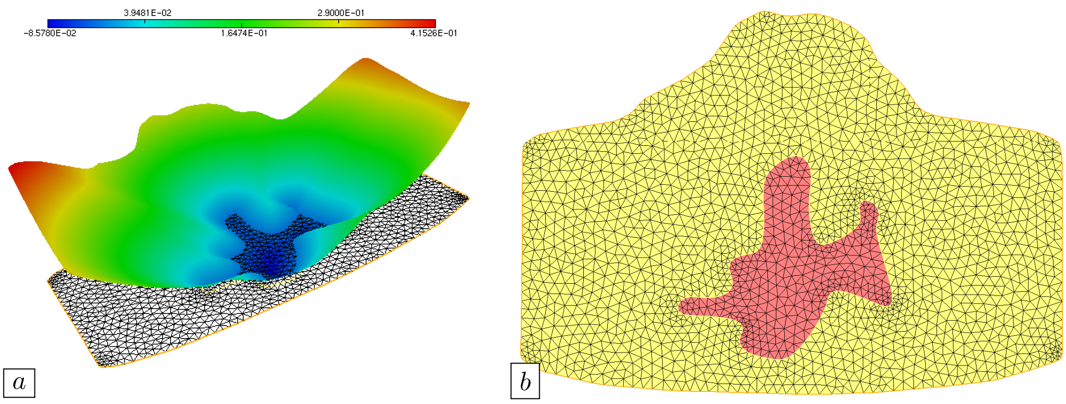

Figure 2. *(a) Graph of a level set function $\phi : D \to \mathbb{R}$ for the cavity Ω; (b) Meshed representation of Ω (in red), as a submesh of the total mesh of D.*

The evolution of a domain $\Omega(t)$ through a velocity field $\mathbf{V}(t,\mathbf{x})$, over a time period $(0,T)$ is conveniently captured in terms of an associated level set function $\phi(t,\cdot)$ (i.e. (7) holds for all $t \in [0,T]$); the latter indeed solves the following advection equation:

$$\forall t \in (0,T),\ \mathbf{x} \in D, \quad \frac{\partial \phi}{\partial t}(t,\mathbf{x}) + \mathbf{V}(t,\mathbf{x}) \cdot \nabla\phi(t,\mathbf{x}) = 0. \tag{8}$$

In this framework, dramatic changes of $\Omega(t)$ can be accounted for, including topological changes, i.e. merging of holes, or creation of holes.

In our application where $\Omega(t)$ is the sought solution of (2), the velocity field is the (negative) descent direction $\boldsymbol{\theta}$ in (6) and the time T stands for the descent step.

2.5 Numerical implementation

Our practical implementation leverages a recent variant of the level set method for shape optimization, introduced in (Allaire et al., 2014) – an open source implementation of which is proposed in (Dapogny & Feppon, 2023). The latter features an additional step at each optimization iteration $n = 0, \ldots$, during which remeshing algorithms are used to create a meshed description of Ω^n, as a submesh of the computational domain D, see Fig. 2

Our numerical workflow is sketched in Alg. 1, and the code is freely available in (Perrot, 2024).

Algorithm 1 Shape optimization algorithm for the reconstruction of a magma chamber.

Initialization: Initial shape $\Omega^0 \subset D$, mesh $\mathcal{T}^0$ of D a submesh $\mathcal{T}^0_{\text{cav}}$ of which accounts for Ω^0.
for $n = 0, ...,$ until convergence **do**
1. Calculate a level set function $\phi^n : D \to \mathbb{R}$ for Ω^n on $\mathcal{T}^n$.
2. Calculate the state $\mathbf{u}_{\Omega^n}$ and adjoint state $\mathbf{p}_{\Omega^n}$ on $\mathcal{T}^n_{\text{cav}}$.
3. Calculate a descent direction $\boldsymbol{\theta}^n$ for J_{LS}, from Ω^n on $\mathcal{T}^n$.
4. Update the level set function by solving the advection equation (8) on $\mathcal{T}^n$.
5. Create a new mesh $\mathcal{T}^{n+1}$ of D in which Ω^{n+1} exists as a submesh.

end for
return Optimized shape $\Omega^n \subset D$ of the cavity.

The initial geometry is created thanks to the open-source software `Gmsh` (Geuzaine et al., 2009). At each iteration n, the computational domain D is discretized by a mesh $\mathcal{T}^n$ which encloses a discretization of the actual shape Ω^n of the magma chamber as a submesh $\mathcal{T}^n_{\text{cav}}$. The state and adjoint systems (1) and (5) for $\mathbf{u}_{\Omega^n}$ and $\mathbf{p}_{\Omega^n}$ are solved on this mesh by the open-source Finite Element library `FreeFem` (Hecht, 2012). A descent direction $\boldsymbol{\theta}^n$ is then obtained by (6), and a level set function ϕ^n for the next iterate Ω^{n+1} is obtained by solving (8) thanks to the open-source library `Advect` (Bui et al., 2012).

3 Validation with synthetic data

To test the method, the idea is to do a kind of cross-validation. On the one hand, we form synthetic observation data from a known source. On the other hand, we initialized the algorithm with a first guess for the source shape and location. We expect the algorithm to iteratively modify the shape of the source and converge to the correct shape and location. In fact, the 3D location of the source (e.g., its center of gravity for a random shape) is not directly optimized as a vector of discrete parameters, but is modified by the simple fact that the boundary is free to move in any direction, and thus can take on a kind of "average rigid body motion" as it gradually moves the center in a given direction.

In practice, the synthetic observed surface displacement field is derived from the McTigue (1987) solution, an analytical approximation of the displacement caused by a uniformly pressurized spherical cavity (the magma domain) embedded in an isotropic, homogeneous, and planar elastic medium (the host crust) with elastic constants tp $E =$ 10GPa and $\mu = 0.25$.

Usually, the quantities to be determined with parametric inversion based on a McTigue model are the location and the radius. The pressure change can also be left as a free parameter, but is interchangeable with the radius, so one must be fixed to determine the other, see Greiner (2021) for more details. For the synthetic source, we fixed these free parameters to $z = -5$km, $\Delta P = 10$MPa, $R = 1.5$km, which are typical values for inverted magmatic domains.

magmaOpt is then allowed to run freely, without any termination condition, to see whether or not it succeeds in converging from the ellipsoid to the McTigue sphere we used to generate the synthetic displacement.

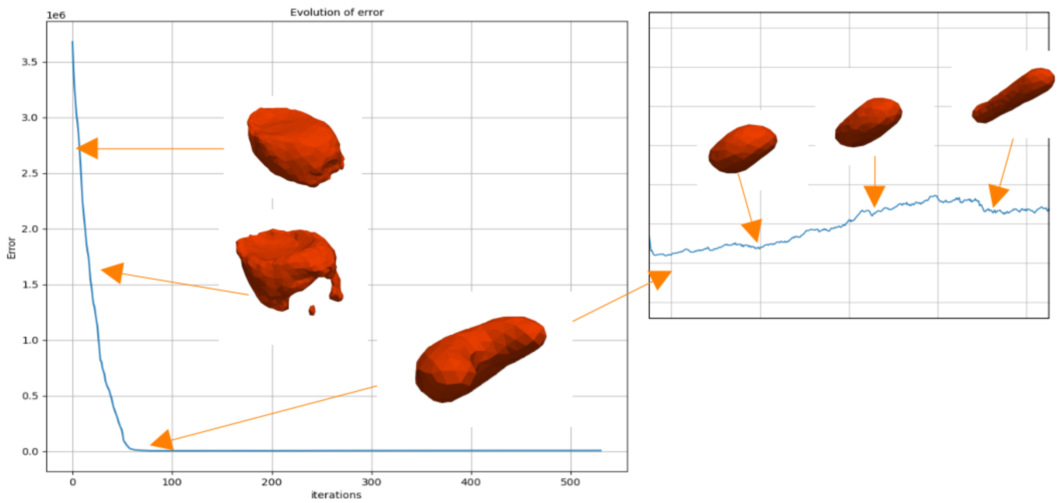

Figure 3. Evolution of error and succesivve shapes taken by the magma source during an optimization loop. The initial guess is a flat ellipsoid of semi-axes $r_x = 2\text{km}, r_y = 3\text{km}, r_z = 1\text{km}$ centered on the true spherical source. The minimum is reached at iteration 82.

As shown in the figure 3, the algorithm seems to converge to a minimum. After that, the slope of the cost function is positive because a small increase in J is allowed. It is obvious that no other minima are found, as the shape evolves towards a stick-shaped feature, far from the expected solution. We can also discuss the minima found. The surface reached is obviously not a sphere, but it is closer than any shape found before. We expect the shape to be closer to a sphere with a finer mesh defined. Many improvements could be realized: for example, once it is obvious that the algorithm will not converge to a better solution, we could restart the algorithm on the best solution found, set new evolution parameters, and allow a finer mesh. By repeating this process automatically, it may be possible to arrive at a more likely shape for the magma reservoir.

4 Real test case : Svartsengi 2022 inflation

We now apply the method to infer the shape of a magma domain in a recent period of volcanic unrest and eruption in SW Iceland by evaluating the shape of a magma body responsible for the ground inflation observed from 21 April to 14 June 2022 at Svartsengi on the Reykjanes peninsula. This is one of 5 inflation episodes that preceded catastrophic dike breaches and eruptions at the Sundhnúkur crater row, which caused the destruction of the city of Grindavík (Sigmundsson et al., 2024).

The observational data used are the line-of-sight (LOS) displacement maps of the area from Cosmo SkyMed available in (Parks et al., 2024), the data used by Sigmundsson et al. (2024). After uniform downsampling and mesh reprojection (the data points must be aligned on the mesh nodes), the ascending A32 and descending D132 tracks were both used in the RMS error function we adapted to the LOS geometry.

$$J(\Omega) = \sum_{i \in tck} \alpha_i \int_{\Gamma_u} \left(L_i(u(x)) - l_o^i(x)\right)^2 dS \tag{9}$$

Where $tck = \{A125, D132\}$. For each track i, α_i is the weight of the track ($\forall i, \alpha_i = 1$ here), $L_i : \mathbb{R}^3 \mapsto \mathbb{R}$ is the function that projects the 3D surface displacement given by the model into the LOS geometry, and l_o^i is the observed LOS displacement.

We then used the framework developed above, only projecting the InSAR data onto the mesh of D and modifying the expression of the error function in `magmaOpt`.

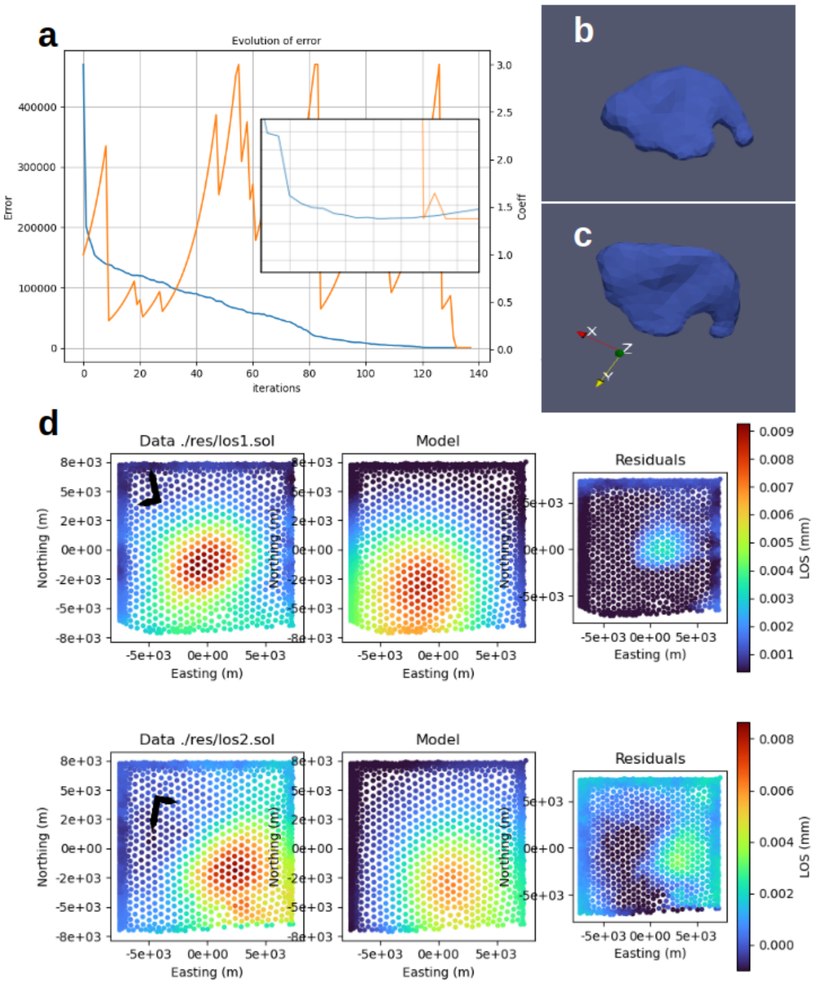

Figure 4. a) Convergence plot with embedded zoom. The blue line is the error and the orange line is the evolution of τ. Minima are reached at iteration 128. b,c) Side and top view of the source Γ_s minimizing J. d) Data, model and residuals of the LOS displacements at iteration 128 for the two InSAR tracks A32 (top) and D132 (bottom). Black arrows are heading and looking directions, coordinates are ISN16 (Valsson, 2019) shifted to a local origin $(2529373E, 179745N)$.

The results shown in figure 4 are encouraging: after providing an initial guess located at the center of inflation at depth for a sphere of radius RR, the algorithm is able to iteratively change the shape and depth of the magma domain to finally result in a sill-like flattened spheroid whose centroid is located at DD depth. This is consistent with the presumed depth found in the supporting information of (?, ?), which performs an analytical model-based inversion. Although the pressure must be fixed, as explained in 1.1, the result can be used to compare the final shape of the magmatic intrusion and give a richer insight into it. Here we see interesting features, such as an increasing thickness on the north side, that can't be traced by any other method. The algorithm produces features that we consider to be artifacts, probably due to mesh refinement problems, such as small holes or horn-shaped features.

5 Discussion

This work paves the way for a new class of methods that tackle an unknown geometry of the magmatic domains, thus giving the possibility to explore irregular shapes that are more likely to exist compared to any other usually assumed regular shapes. However, even if the first results presented are promising, many questions remain to be answered. First of all, the internal pressure of the chamber must be specified, which is a strong hypothesis. In this context, the precise shape of the source should be determined as a second step. The traditional analytical model-based inversion would be run first, giving a pressure and a first educated guess for the position and shape of Ω_0. Then a more realistic shape could be sought with a shape optimization taking the output of the inversion as an initial guess.

Adding constraints may also be an interesting way to explore. For example, the volume of the source could be constrained to be within bounds or even to match a certain value. The implemented shape optimization is certainly able to handle constraints as described by Allaire et al. (2021). The physical meaning of the best shape might benefit from a more constrained problem, and the less influencing deeper part of the source might be less random.

To better understand the influence of data partitioning and variablitiy, additional tests could be run with synthetic data. We can think of tests such as masking part of the surface displacement field, introducing noise and parasitic signals, reducing the number of data points, as is often the case in reality with areas of volcanic systems lacking data coverage (glacier, river, lava, forest) and subjected to perturbations (atmospheric distortion, weather).

It is also important to mention that the behavior of the algorithm is influenced by numerous parameters of varying importance, starting from the discretization length (element size) or the domain extent, to the limits of the step size τ, the regularization length, or the number of iterations allowed by the line search. A systematic study of each of these parameters would be beneficial in assessing the quality of the shape inferred.

Exploring a way to quantify the uncertainty of the answer is also crucial. For example, a sensitivity analysis approach could be considered, as well as the inclusion of a probabilistic quantity.

6 Conclusion

The present study has successfully demonstrated the application of inverse problems and computational methods to infer the shape of a magma domain beneath a volcano using ground inflation data from satellite observations. The shape optimization technique used in this research showed a new way to identify the most likely shape of the magma chamber. It was intended as an opening to new methods rather than a complete solution.

We have shown that modifying a shape optimization algorithm to handle geophysical problems is feasible and of interest. Tests on synthetic data showed to some extent the relevance of the approach, although the best sources found exposed the limitations faced by these first attempts of shape optimization for volcano geodesy. The test on real data showed a concrete case of how the method could be used after being more mature.

The perspectives are numerous. The numerical nature of the models allows to easily add complexities to the modeling, such as complex mechanical behavior of the crust (plaxticity, viscoelasticity, poroelsaticity), additional loads (tectonic stress, tidal loads, glacier weights), or inhomogeneities. We hope that the open source code `magmaOpt` developed by us will be modified and extended by future work.

By addressing these limitations and extending this approach, researchers can further improve the accuracy and reliability of magma domain shape inference. Ultimately, the development of more sophisticated models will enable geophysicists to better monitor volcanic activity, predict eruptions, and provide critical support for hazard mitigation strategies.

Open Research Section

This section MUST contain a statement that describes where the data supporting the conclusions can be obtained. Data cannot be listed as "Available from authors" or stored solely in supporting information. Citations to archived data should be included in your reference list. Wiley will publish it as a separate section on the paper's page. Examples and complete information are here: https://www.agu.org/Publish with AGU/Publish/Author Resources/Data for Authors

As Applicable – Inclusion in Global Research Statement

The Authorship: Inclusion in Global Research policy aims to promote greater equity and transparency in research collaborations. AGU Publications encourage research collaborations between regions, countries, and communities and expect authors to include their local collaborators as co-authors when they meet the AGU Publications authorship criteria (described here: https://www.agu.org/publications/authors/policies#authorship). Those who do not meet the criteria should be included in the Acknowledgement section. We encourage researchers to consider recommendations from The TRUST CODE - A Global Code of Conduct for Equitable Research Partnerships (https://www.globalcodeofconduct.org/) when conducting and reporting their research, as applicable, and encourage authors to include a disclosure statement pertaining to the ethical and scientific considerations of their research collaborations in an "Inclusion in Global Research Statement' as a standalone section in the manuscript following the Conclusions section. This can include disclosure of permits, authorizations, permissions and/or any formal agreements with local communities or other authorities, additional acknowledgements of local help received, and/or description of end-users of the research. You can learn more about the policy in this editorial. Example statements can be found in the following published papers: Holt et al. (https://agupubs.onlinelibrary.wiley.com/doi/full/10.1029/2022JG007188), Sánchez-Gutiérrez et al. (https://agupubs.onlinelibrary.wiley.com/doi/abs/10.1029/2023JG007554), Tully et al. (https://agupubs.onlinelibrary.wiley.com/doi/epdf/10.1029/2022JG007128) Please note that these statements are titled as "Global Research Collaboration Statements" from a previous pilot requirement in JGR Biogeosciences. The pilot has ended and statements should now be titled "Inclusion in Global Research Statement".

Acknowledgments

Enter acknowledgments here. This section is to acknowledge funding, thank colleagues, enter any secondary affiliations, and so on.

References

Allaire, G. (2006). *Conception optimale de structures* (Vol. 58). Springer Berlin Heidelberg. doi: 10.1007/978-3-540-36856-4

Allaire, G., Dapogny, C., & Frey, P. (2014). Shape optimization with a level set based mesh evolution method. *Computer Methods in Applied Mechanics and Engineering*, *282*, 22–53.

Allaire, G., Dapogny, C., & Jouve, F. (2021). Chapter 1 - Shape and Topology Optimization. In A. Bonito & R. H. Nochetto (Eds.), *Geometric Partial Differential Equations - Part II* (Vol. 22, pp. 1–132). Elsevier. doi: 10.1016/bs.hna.2020.10.004

Allaire, G., Jouve, F., & Toader, A.-M. (2004). Structural optimization using sensitivity analysis and a level-set method. *Journal of computational physics*, *194*(1), 363–393.

Andreassen, E., Clausen, A., Schevenels, M., Lazarov, B. S., & Sigmund, O. (2011, January). Efficient Topology Optimization in MATLAB Using 88 Lines of Code. *Structural and Multidisciplinary Optimization*, *43*(1), 1–16. doi: 10.1007/s00158-010-0594-7

Bagnardi, M., & Hooper, A. (2018, July). Inversion of Surface Deformation Data for Rapid Estimates of Source Parameters and Uncertainties: A Bayesian Approach. *Geochemistry, Geophysics, Geosystems*, *19*(7), 2194–2211. doi: 10.1029/2018GC007585

Bendsoe, M. P., & Sigmund, O. (2004). Topology Optimization by Distribution of Isotropic Material. In M. P. Bendsoe & O. Sigmund (Eds.), *Topology Optimization: Theory, Methods, and Applications* (pp. 1–69). Berlin, Heidelberg: Springer. doi: 10.1007/978-3-662-05086-6_1

Bui, C., Dapogny, C., & Frey, P. (2012). An accurate anisotropic adaptation method for solving the level set advection equation. *International Journal for Numerical Methods in Fluids*, *70*(7), 899–922.

Cea, J. (1986). Conception Optimale Ou Identification de Formes, Calcul Rapide de La Dérivée Directionnelle de La Fonction Coût. *ESAIM: Modélisation mathématique et analyse numérique*, *20*(3), 371–402.

Cervelli, P., Murray, M. H., Segall, P., Aoki, Y., & Kato, T. (2001). Estimating Source Parameters from Deformation Data, with an Application to the March 1997 Earthquake Swarm off the Izu Peninsula, Japan. *Journal of Geophysical Research: Solid Earth*, *106*(B6), 11217–11237. doi: 10.1029/2000JB900399

Charco, M., & Galán del Sastre, P. (2014, March). Efficient Inversion of Three-Dimensional Finite Element Models of Volcano Deformation. *Geophysical Journal International*, *196*(3), 1441–1454. doi: 10.1093/gji/ggt490

Dapogny, C., & Feppon, F. (2023, October). Shape Optimization Using a Level Set Based Mesh Evolution Method: An Overview and Tutorial. *Comptes Rendus. Mathématique*, *361*(G8), 1267–1332. doi: 10.5802/crmath.498

Dzurisin, D. (2007). *Volcano Deformation: Geodetic Monitoring Techniques.* Berlin ; New York : Chichester, UK: Springer ; Praxis.

Feppon, F., Allaire, G., Dapogny, C., & Jolivet, P. (2020, September). Topology Optimization of Thermal Fluid–Structure Systems Using Body-Fitted Meshes and Parallel Computing. *Journal of Computational Physics*, *417*, 109574. doi: 10.1016/j.jcp.2020.109574

Frei, W. (2015, December). *Designing New Structures with Shape Optimization.* https://www.comsol.com/blogs/designing-new-structures-with-shape-optimization. COMSOL.

Geuzaine, C., Remacle, J.-F., & Dular, P. (2009). Gmsh: A Three-Dimensional Finite Element Mesh Generator. *International Journal for Numerical Methods in Engineering*, *79*(11), 1309–1331.

Greiner, S. H. (2021). *Including Topography and a 3D-elastic Structure into a Finite-Element Deformation Model of Grímsvötn, Iceland* (Unpublished doctoral dissertation).

Hecht, F. (2012). New Development in FreeFem++. *Journal of Numerical Mathematics*, *20*(3-4), 251–265.

Henrot, A., & Pierre, M. (2018). *Shape variation and optimization.* EMS Tracts in Mathematics Vol. 28.

Hickey, J., & Gottsmann, J. (2014, June). Benchmarking and Developing Numerical Finite Element Models of Volcanic Deformation. *Journal of Volcanology and Geothermal Research*, *280*, 126–130. doi: 10.1016/j.jvolgeores.2014.05.011

Hunter, W., et al. (2017). *ToPy - Topology Optimization with Python.* GitHub.

Le Quilliec, G. (2014). Topology Optimization Procedure TOPOPTIM and Other Various Developments Made with Cast3M. doi: 10.13140/2.1.2718.3682

Lucchini, F., Torchio, R., Cirimele, V., Alotto, P., & Bettini, P. (2022). Topology optimization for electromagnetics: A survey. *IEEE Access*, *10*, 98593–98611.

McTigue, D. F. (1987, November). Elastic Stress and Deformation near a Finite Spherical Magma Body: Resolution of the Point Source Paradox. *Journal of Geophysical Research: Solid Earth*, *92*(B12), 12931–12940. doi: 10.1029/JB092iB12p12931

Mogi, K. (1958). Relations between the Eruptions of Various Volcanoes and the Deformations of the Ground Surfaces around Them. *Earthq Res Inst*, *36*, 99–134.

Murat, F., & Simon, J. (1976). Sur le contrôle par un domaine géométrique. *Pré-publication du Laboratoire d'Analyse Numérique,(76015).*

Osher, S., & Fedkiw, R. (2006). *Level set methods and dynamic implicit surfaces* (Vol. 153). Springer Science & Business Media.

Parks, M., Drouin, V., Geirsson, H., Hooper, A., Hreinsdóttir, S., Ófeigsson, B., ... Tolpekin, V. (2024, January). Data and Geodetic Modelling Results for Science Article "Fracturing and Tectonic Stress Drives Ultra-Rapid Magma Flow into Dikes".

Perrot, T. (2024). *magmaOpt.* Retrieved from `https://github.com/`

Plessix, R.-E. (2006). A review of the adjoint-state method for computing the gradient of a functional with geophysical applications. *Geophysical Journal International*, *167*(2), 495–503.

Sethian, J. A. (1999). *Level set methods and fast marching methods: evolving interfaces in computational geometry, fluid mechanics, computer vision, and materials science* (Vol. 3). Cambridge university press.

Sigmund, O. (2001, April). A 99 Line Topology Optimization Code Written in Matlab. *Structural and Multidisciplinary Optimization*, *21*(2), 120–127. doi: 10.1007/s001580050176

Sigmund, O., & Maute, K. (2013, December). Topology Optimization Approaches: A Comparative Review. *Structural and Multidisciplinary Optimization*, *48*(6), 1031–1055. doi: 10.1007/s00158-013-0978-6

Sigmundsson, F., Parks, M., Geirsson, H., Hooper, A., Drouin, V., Vogfjörd, K. S., ... Barsotti, S. (2024, February). Fracturing and Tectonic Stress Drives Ultrarapid Magma Flow into Dikes. *Science*, eadn2838. doi: 10.1126/science.adn2838

Slavov, S., & Konsulova-Bakalova, M. (2019, January). Optimizing Weight of Housing Elements of Two-stage Reducer by Using the Topology Management Optimization Capabilities Integrated in SOLIDWORKS: A Case Study. *Machines*, *7*(1), 9. doi: 10.3390/machines7010009

Taylor, N. C., Johnson, J. H., & Herd, R. A. (2021, November). Making the Most of the Mogi Model: Size Matters. *Journal of Volcanology and Geothermal Research*, *419*, 107380. doi: 10.1016/j.jvolgeores.2021.107380

Trasatti, E. (2022, July). Volcanic and Seismic Source Modeling: An Open Tool for Geodetic Data Modeling. *Frontiers in Earth Science*, *10*. doi: 10.3389/feart

.2022.917222

Valsson, G. Þ. (2019, March). *ISN2016 - Tækniskýrsla* (Tech. Rep.). Íslands: Landmælingar.

Velez, M. L., Euillades, P., Caselli, A., Blanco, M., & Díaz, J. M. (2011, April). Deformation of Copahue Volcano: Inversion of InSAR Data Using a Genetic Algorithm. *Journal of Volcanology and Geothermal Research*, *202*(1), 117–126. doi: 10.1016/j.jvolgeores.2011.01.012

Yang, X.-M., Davis, P. M., & Dieterich, J. H. (1988). Deformation from Inflation of a Dipping Finite Prolate Spheroid in an Elastic Half-Space as a Model for Volcanic Stressing. *Journal of Geophysical Research: Solid Earth*, *93*(B5), 4249–4257. doi: 10.1029/JB093iB05p04249